

Effect of Step Edge Transition Rates and Anisotropy in Simulations of Epitaxial Growth

E. Chason and B.W. Dodson

SAND--90-1239C

Sandia National Laboratories, Albuquerque, NM 87185

DE91 001251

Abstract

We present the results of a hybrid rate equation/Monte Carlo simulation of epitaxial growth on vicinal surfaces. We have studied the effect on surface morphology of changing transition rates at step edges, of changing detachment rates from step edges and clusters, and of adding anisotropy to the diffusion and incorporation kinetics at step edges and islands. The effect of the transition rates on surface morphology are discussed in terms of a balance between growth by nucleation and coalescence of islands and by the propagation of steps.

Received by SNT
OCT 2 1990

DISCLAIMER

This report was prepared as an account of work sponsored by an agency of the United States Government. Neither the United States Government nor any agency thereof, nor any of their employees, makes any warranty, express or implied, or assumes any legal liability or responsibility for the accuracy, completeness, or usefulness of any information, apparatus, product, or process disclosed, or represents that its use would not infringe privately owned rights. Reference herein to any specific commercial product, process, or service by trade name, trademark, manufacturer, or otherwise does not necessarily constitute or imply its endorsement, recommendation, or favoring by the United States Government or any agency thereof. The views and opinions of authors expressed herein do not necessarily state or reflect those of the United States Government or any agency thereof.

DISTRIBUTION OF THIS DOCUMENT IS UNLIMITE
gpa

I. Introduction

Images of crystal surfaces after controlled amounts of deposition [1,2,3] have given us tremendous insight into the kinetics of crystal growth from the vapor phase. The surface morphology after deposition is the result of the interaction among multiple processes. The richness of the observed morphologies indicates the complexity of the interactions controlling surface evolution. The processes of adatom deposition, surface diffusion, nucleation of islands and detachment from steps and islands contribute to determining the surface morphology in varying degrees based on their relative rates of occurrence. To add to the complexity, it appears that both surface diffusion and attachment to islands may be anisotropic on dimerized (001) semiconductor surfaces [4,5].

In this work, we present the results of simulations of epitaxial growth on vicinal surfaces which demonstrate how changing the relative rates of certain surface processes affects the surface morphology. In particular, we examine two major effects which we believe are relevant to the case of semiconductor growth. In the first, we examine the influence of changing transition rates at step edges both in terms of diffusion up and down steps and detachment of atoms from steps. The strong influence of these parameters on surface roughness and island shape may be relevant to the observation that even small amounts of impurities during growth can greatly affect surface morphology. In the second case, we examine the effect of

anisotropy in both surface diffusion and adatom incorporation into islands. This "dimer-string"-like [4] mode of growth reproduces many of the features observed in STM images of Si grown on Si (001). In addition, we demonstrate that anisotropic island shapes can be obtained from anisotropy in either diffusion or in island incorporation, though the latter leads to much greater shape anisotropy.

II. Computer Simulation

These simulations are based on a hybrid rate equation/Monte Carlo scheme developed in our laboratory [6] and independently by Maksym [7]. In this approach, we do not monitor the state of every site on the surface but instead keep lists of all the candidates in particular configurations on the surface which may undergo a transition; to each possible configuration (18 in all) we assign a transition rate. The lists encompass all the adatoms on the surface and all non-fully coordinated members of islands (i.e. less than 4 nearest neighbors). A schematic of the various surface processes considered is shown in figure 1. The rates for adatom diffusion, jumps up and down steps, jumps toward and away from islands, detachment from islands of 1-, 2- and 3-coordinated atoms and deposition are all independently variable.

For simplicity, we assume the processes are thermally activated and assign an activation energy to each one. The choices of energy were guided by molecular dynamics simulations, the results of which indicated anisotropic diffusion on the Si (001) surface has an activation energy of 0.8 eV along the

fast diffusion direction (parallel to the dimer rows) and 1.2 eV along the slow direction (normal to the dimer rows). Other activation energies were estimated based on their difficulty relative to these two processes. The attempt frequency (f) for all the configurations was chosen as 10^{12} /s; the deposition rate for all the simulations discussed here is .1 monolayers/s. Obviously, we do not know the activation energies for all these processes exactly. However, we do not intend the results expressed here to conform rigorously to real Si. Rather, we hope to demonstrate that changes in the *relative* transition rates can have large effects on the surface morphology.

The nominal values of the energies used for each transition are given in table 1 for the separate cases of isotropic and anisotropic incorporation. By anisotropic incorporation, we mean that an adatom may only be incorporated into the end of a dimer string. In the isotropic case, the adatom may be incorporated into any side of an existing cluster. The energies given in the table represent the values used unless a variation is discussed in the text.

Events are chosen from the lists of possible candidates based on the relative probability of that particular event. There is a separate list for each type of configuration; each member of the list points back to a location on the surface where that configuration exists. The rate of any individual surface transition (indexed by i) occurring is

$$r_i = N_i f \exp(-E_i/kT) \quad (1)$$

where N_i is the number of candidates in the i th configuration and E_i is the activation energy. The total rate (R) of any process occurring (including

deposition) is

$$R = \phi + \sum_i r_i \quad (2)$$

where ϕ is the deposition rate. The type of event is then chosen randomly with the probability of choosing any configuration weighted by r_i/R and the probability of choosing deposition being ϕ/R . The time step associated with each event is $1/R$. Once the particular type of event is chosen, a candidate is chosen randomly from the list of sites in that configuration (or in the case of deposition, a surface site is chosen randomly). The type of event is **executed**, e.g. a diffusive jump, and the **surface** and lists of configurations are updated to reflect the new surface configuration. Then, the new relative transition probabilities are calculated and a candidate is chosen again. Pointers from the surface positions back to the configuration lists are maintained in order to optimize the updating when the surface configuration changes after each event.

The benefits of this approach are that every iteration of the computational loop corresponds to what we consider an "interesting" event such as diffusion, deposition or detachment. In standard Monte Carlo strategies [8], in comparison, an atomic site is chosen randomly and then the probability of that site undergoing a transition is determined. Many iterations then correspond to "null" events, e.g. no diffusive jump. The independence of events is determined by the dilute number of adatoms on the surface; we do not allow for the possibility of correlated events.

The starting surface consisted of an array of 64×128 atoms arranged

on three terrace heights separated by two single atom high steps. Periodic boundary conditions were used, so that atoms which diffused off one terrace edge re-appeared on the opposite side of the array. An even number of steps was required for the studies of anisotropic growth so that the boundaries of even numbered surfaces matched up properly. The two even numbered starting layers had 64×32 atoms and the single odd-numbered layer had 64×64 atoms, so the number of atoms on each type of starting surface was identical.

Although this simulation is intended to be relevant to Si (001) growth, we do not consider the motion of individual monomers on the surface. Rather, we approximate the dimerized nature of the surface (in the section on anisotropic growth) in terms of the anisotropic diffusion and anisotropic incorporation at dimer string ends. We thus do not treat the full complexity of growth on (001) surfaces, neglecting, for instances, the association of monomers to form dimers or the possibility of anti-phase boundaries forming. We only approximate this situation by treating our diffusing species with the same rules that we expect to apply for monomer diffusion and the transition rates as if there is a single rate-determining step which determines the kinetics of dimer growth.

III. Isotropic Growth

Results of the simulation for the case of isotropic diffusion and isotropic incorporation are shown in figure 2 after .5 monolayers of

deposition. The growth temperatures of 500 C, 600 C and 700 C are indicated on the figure; lighter shades on the surface represent increasing atomic level. As the growth temperature is increased, note the dramatic change in surface morphology after 0.5 monolayers of deposition. At low temperature (500 C), the island shapes are snowflake-like and uniformly distributed along the terrace. The steps have not moved from their original position and multiple islands are growing on the terrace. At the intermediate temperature (600 C), the individual islands are larger, fewer in number, and their shapes are more amorphous. The terrace ledges have moved forward relative to their starting position. At even higher temperatures (700 C) there is no nucleation of islands in front of the step edge at all; the growth proceeds purely by step flow.

The temperature dependence of the surface morphology may partially be understood in terms of competition between step flow and nucleation/coalescence of islands. This is seen more clearly in the cross-sections of the surfaces shown under each picture in figure 2. The solid line represents an average across the surface of the atomic height taken in a direction parallel to the step edges. The dashed line represents where the step edge would be if the growth proceeded purely by step flow. In the low temperature case (500 C) after 0.5 monolayers of deposition, note how the step edge of the dashed line (representing step flow) is roughly halfway between the actual steps on the surface; there is no indication that the step has moved. At higher temperatures (600 C), note how the edge of the dashed line is closer to the back step than the front step indicating this step

has moved forward relative to the starting surface. At 700 C, the step front moves forward at the same rate as the dashed line. All deposited adatoms diffuse to step edges; small clusters which do occasionally form do not grow large enough to be stable and eventually succumb to disintegration.

The time evolution of the surface in the intermediate temperatures of our simulation where both nucleation/coalescence and step flow occur is very interesting to observe. In the early stages of growth, before any nucleation of islands occurs, the step starts to advance. Subsequently, some nucleation occurs in a region ahead of the step leaving a denuded zone (as referred to by Lagally [5]) between the **step edge** and the nucleation region corresponding to the diffusion length of the adatoms. As these islands begin to grow, the **advance of the step is retarded** as the newly nucleated islands compete with the existing steps for adatoms. The nucleation occurs very non-uniformly. After the initial burst of nucleation on the flat terrace at some distance ahead of the step edge, the new islands become sinks for adatoms and reduce the concentration of adatoms on the surface so that no more nucleation occurs. Island growth and coalescence effectively stops any further nucleation, and for that matter any more significant step flow, until the terrace is nearly completely filled in. At that point, there is another burst of nucleation and the process is repeated. This burst of nucleation has been predicted by Stoyanov [9] and appears to be demonstrated by our simulation.

IV. Effect of Step Edge Reflection and Detachment Energy on Isotropic

Growth

In the preceding section, the energy to diffuse down step edges is taken to be the same as for diffusion on the same level (there is effectively no up-diffusion since every adatom arriving at an atomic step is incorporated into the step). In this section, we examine the effect of increasing the energy to go down an atomic step by 0.2 eV relative to diffusion on the same level; this is accomplished by increasing the energies of configurations 7 through 13 in table 1 by 0.2 eV. This is analogous to making adatoms partially reflect from step edges.

The results of this change are shown in figure 3 at a growth temperature of 600 C after 1.0 monolayer of deposition. The surface morphology is clearly rougher than when there is no step edge reflection. The layer is unable to fill in and become smooth again since as the islands coalesce there is less and less likelihood of adatoms landing between the islands. Instead, nucleation on top of the islands is enhanced. In the cross-sectional view of the surface, there is enhanced nucleation directly above the step edge. In the case of no step-edge reflection, the region above the step edge was a denuded zone (figure 1c), as adatoms which spilled over were incorporated into the moving edge. At even larger values of the step edge reflection, we observe a density spike directly above the step edge from the extra nucleation induced by the excess concentration of adatoms near the step edge.

The effect of decreasing the energy of detachment from step edges and

island sides, or equivalently, of increasing the ripening kinetics, is shown in figure 4 for growth at 500 C. This surface was grown under similar conditions to that shown in figure 2a but with all the detachment energies (configurations 14 - 18 in table 1) decreased by 0.2 eV. The effect on the island shape is dramatic, changing from a snowflake-like rough shape to more amorphous smooth-edged shapes. The apparent number of nuclei decreases dramatically as the lower detachment energy makes it possible for small nuclei to disintegrate and aid in the ripening of larger islands. The increased detachment rate adds slightly to the rate of step flow as well, coincident with the appearance of a denuded zone above the step edge.

The results of changing these transition rates at step edges demonstrate how effects which occur on only a small fraction of the surface may have a large effect on the evolution of the surface morphology. We chose to concentrate on step edges because of the tendency for certain impurities to incorporate preferentially at these sites. Although the step edges represent a small fraction of the surface, clearly changing the transition rates there can have a dramatic effect on the growth. This may be relevant to the observation during molecular beam epitaxy that even small amounts of impurities on the surface can dramatically alter the growth [10]. In fact, the continual decrease in epitaxial growth temperatures over the last decade may be partially due to the coincident increase in the cleanliness of the conditions under which they are grown. We speculate that the observation of improved epitaxial growth on miscut surfaces relative to nominally oriented [11] may be due to the higher density of steps reducing global impurity

poisoning of the growth process.

V. Anisotropic Diffusion and Isotropic Growth

It is apparent from images obtained with the scanning tunneling microscope (STM) that growth on Si (001) surfaces is highly anisotropic. This anisotropy rotates by 90 deg with each layer height in correspondence with the direction of the dimer bond on the 2x1 reconstructed surface. We have shown in earlier work that anisotropic incorporation of adatoms into islands can lead to anisotropic island shapes [4]. In this section, we examine the effect of making the surface diffusion anisotropic while still keeping the incorporation into the island isotropic.

We add anisotropy to the diffusional kinetics by increasing the activation energy in the "slow" diffusional direction from 0.8 eV to 1.2 eV. We increase all the other diffusional energies which require a jump in this direction by the same amount; detachment energies are left unchanged. The direction of "slow" diffusion rotates by 90 deg on each successive layer.

The surface after 0.5 monolayers of growth at 500 C is shown in figure 5. The island shapes are anisotropic, though not nearly so much as in the case of anisotropic incorporation. However, it appears that shape anisotropy can in fact be induced purely by diffusional anisotropy and does not strictly imply anisotropy in the island incorporation. Most significantly, the direction of fast surface diffusion (perpendicular to the direction of the dimer bonds in the underlying layer) is perpendicular to the long-axis of the islands. This

relationship between shape anisotropy and diffusional anisotropy is the same as that determined by Lagally [5] from STM images of MBE grown Si on Si (001). The shape anisotropy induced by anisotropic diffusion is thus in the same direction as that induced by anisotropic incorporation at the end of dimer strings; both effects tend to enhance the island growth parallel to the underlying dimer bonds (normal to the underlying dimer rows). At higher temperatures, we observe a decrease in the shape anisotropy which we attribute to increased ripening of the islands.

VI. Anisotropic Incorporation and Anisotropic Diffusion

In this section we examine the effect of anisotropic diffusion and anisotropic incorporation on surface morphology. Adding anisotropy to the simulation vastly complicates the interactions which occur between the different growth modes of nucleation/coalescence and step propagation. Since the anisotropy breaks the symmetry between steps on odd and even layers, it is no longer sufficient to consider growth on only one terrace of the surface. As discussed in the preceding section, the fast diffusion direction is taken as normal to the dimer bond in the underlying layer. Incorporation into the growing dimer string is only allowed at the end of the string; the string ends propagate in a direction parallel to the underlying dimer bond.

The temperature dependence of the surface morphology after 0.5 monolayers of growth under conditions of anisotropic diffusion and anisotropic incorporation (with energies given in figure 1 for the "anisotropic

case") is shown in figure 6. The anisotropy in island shape is apparent even at the lowest temperature (500 C) where the rate of diffusion is lowest. The difference in growth mode between anisotropic and isotropic incorporation is not as easy to see. As the temperature is raised, the rate of diffusion of adatoms to the steps increases just as in the case of isotropic growth. However, in this case, only one of the steps is able to incorporate the arriving adatoms into the step, the one with the ends of the dimer strings forming the step. The other step, with the dimer string parallel to the step edge, can not incorporate any adatoms. The only way in which growth can occur on the terrace in front of this step is by nucleation of new dimer strings on the terrace. At low temperatures, where nucleation and coalescence of new dimer strings is dominant and step flow is insignificant, this asymmetry is unimportant and the two terrace ledges grow independently while maintaining roughly equal sizes. At higher temperatures, however, where step propagation dominates the fast growing step overruns the slow growing step. However, the fast growing step can not proceed when it reaches a double step and so must wait for the underlying slow-growing step to complete before growth may proceed. As temperature increases, therefore, we see an increase in the size of the terrace on which dimer strings can grow quickly and a decrease in the size of the terrace on which they must nucleate. At even higher temperatures, the surface grows primarily by double-step propagation, with the end of the fast growing step being coincident with the end of the slow growing step.

VII. Conclusion

We have developed Monte Carlo simulations to study the effect of varying the transition rates of certain surface processes on the evolution of surface morphology during epitaxial growth on vicinal surfaces. By changing the growth temperature (i.e., increasing surface diffusion rates relative to the deposition rate), we observe a transition from nucleation and coalescence of islands on the terrace to step propagation. In this transition region, the nucleation of islands is non-uniform spatially and temporally. The islands nucleate ahead of the moving step front in a burst of nucleation; the subsequent coalescence of these islands decreases the adatom population on the surface thus effectively cutting off any further nucleation. Capture of adatoms by the islands retards further step flow. We have further shown that changing the transition rates at step edges (of up/down diffusion and detachment) has a dramatic effect on the surface morphology.

We have also investigated the effect of anisotropy in diffusion and island incorporation on the evolution of surface morphology. Anisotropy in the diffusion alone (with isotropic incorporation) is sufficient to create anisotropy in the island shape, though not as great as anisotropic incorporation. In the case of anisotropic diffusion and anisotropic incorporation, the inequivalence of the two types of steps leads to the fast growing terrace overrunning the slow growth terrace. In the extreme of high temperature, the growth proceeds by the propagation of double-height steps.

Acknowledgments

We thank J.Y. Tsao, T. Klitsner, K.M. Horn, P. Taylor, B.L. Doyle and P. Bedrossian for useful discussion and assistance. This work was performed at Sandia National Laboratories, supported by the U. S. government under contract DE-AC04-76DP00789.

References

1. R.J. Hamers, U.K. Kohler and J.E. Demuth, *Ultramicroscopy* 31 (1989) 10.
2. Y.-W. Mo, R. Kariotis, B.S. Schwartzentuber, M.B. Webb and M.G. Lagally, *J. Vac. Sci. Technol.* A8 (1990) 201.
3. A. J. Hoeven, D. Dijkkamp, E.J. van Loenen, M. Lenssinck and J. Dieleman, *J. Vac. Sci. Technol.* A8 (1990) 207.
4. J.Y. Tsao, E. Chason, U. Koehler and R. Hamers, *Phys. Rev.* B40 (1989) 11951.
5. Y.-W. Mo and M.G. Lagally, submitted to *Surf. Sci.*
6. E. Chason and J.Y. Tsao, *Surf. Sci.*, in press.
7. P.A. Maksym, *Semicind. Sci. Technol.* 3 (1988) 594.
8. F.F. Abraham and G.M. White, *J. of Appl. Phys.* 41 (1970) 1841.
9. S. Stoyanov and M. Michailov, *Surf. Sci.* 202 (1988) 109.
10. J.C. Bean, *J. of Cryst. Growth* 70 (1985) 444.
11. still need to find reference

Figure Captions

Figure 1. Schematic of the surface representing the different configurations considered in the simulation. Energies used to calculate each transition rate are given in table 1.

Figure 2. Representations of surfaces after undergoing 0.5 monolayers of growth in the isotropic mode. Simulation growth temperatures are: a) 500 C, b) 600 C and c) 700 C. In the schematics of the surface, lighter shades represent higher levels. Underneath the surfaces are representations of the atom density in cross-section (solid line) and the calculated position of the steps if all the growth proceeded by step flow.

Figure 3. Effect of increasing step edge diffusion energy on surface morphology. Schematic of surfaces represent morphology after 1.0 monolayer of growth at 600 C for a) nominal diffusion values and b) increased energy for diffusion down steps. Cross-section of surface shown below schematic.

Figure 4. Effect of decreasing step edge detachment energy on surface morphology. Schematic of surface represents morphology after 0.5 monolayers of deposition at 500 C. Cross-section of surface shown below schematic.

Figure 5. Effect of adding anisotropy to surface diffusion on surface morphology. Schematic of surface represents morphology after 0.5 monolayers of growth at 500 C. The fast diffusion direction rotates 90 deg with each successive layer. The activation energy is 0.8 eV for fast diffusion and 1.2 eV for slow diffusion.

Figure 6. Temperature dependence of surfaces grown under conditions of anisotropic incorporation and anisotropic diffusion. Schematic of surface represents morphology after 0.5 monolayers of growth at a) 500 C, b) 600 C and c) 700 C.

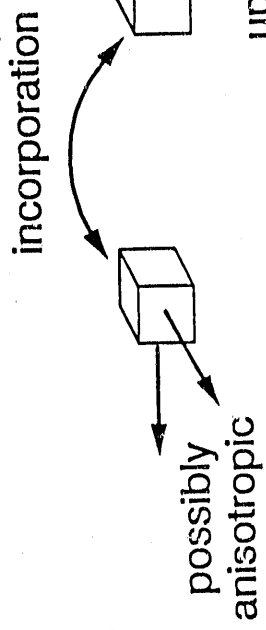
Table 1

energy (in eV) for:	anisotropic case	isotropic case
diffusional jump	.8 (fast) 1.2 (slow)	.8
jump toward side of string (island)	.8	.8
jump away from side of string	.9	-
jump toward end of string (island)	1.1	.8
jump up side of string	1.2	-
jump down side of string (island)	1.2	.8
jump down end of string (island)	1.0	.8
jump up double step	1.6	.8
jump down double step	1.6 (slow) 1.0 (fast)	.8
jump up triple step (or higher)	1.6	.8
jump down triple step (or higher)	1.6	.8
detachment from 1-coordinated site	1.2	1.2
detach from 2-coordinated site	1.2 (string end and side) 1.4 (2 string ends)	1.4
detach from 3-coordinated site	1.5 (string end and 2 sides) 1.4 (string side and 2 ends)	1.6

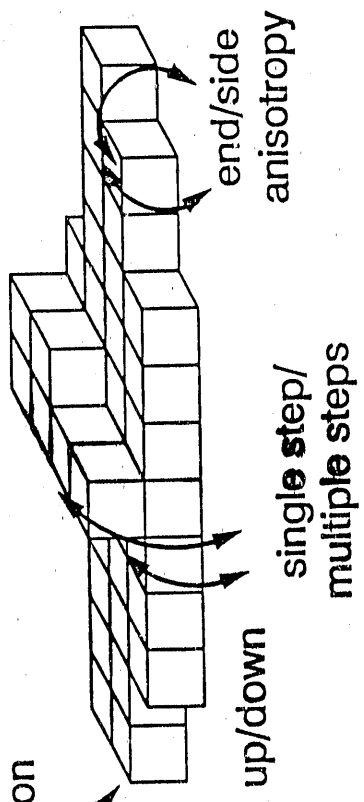
(-) indicates this type jump not possible on that surface or is configuration dependent.

Energies for Computing Relative Rates

Intralayer diffusion



Interlayer diffusion



Detachment

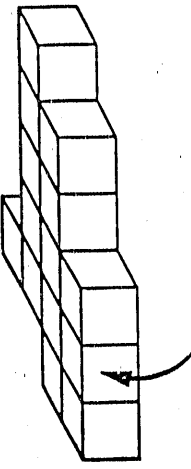
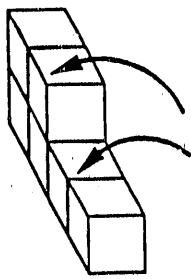
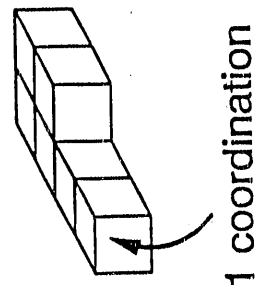


figure 1

Chason and Dodson
file: simul1.drw
8/14/90

Isotropic Incorporation (0.5 monolayers)

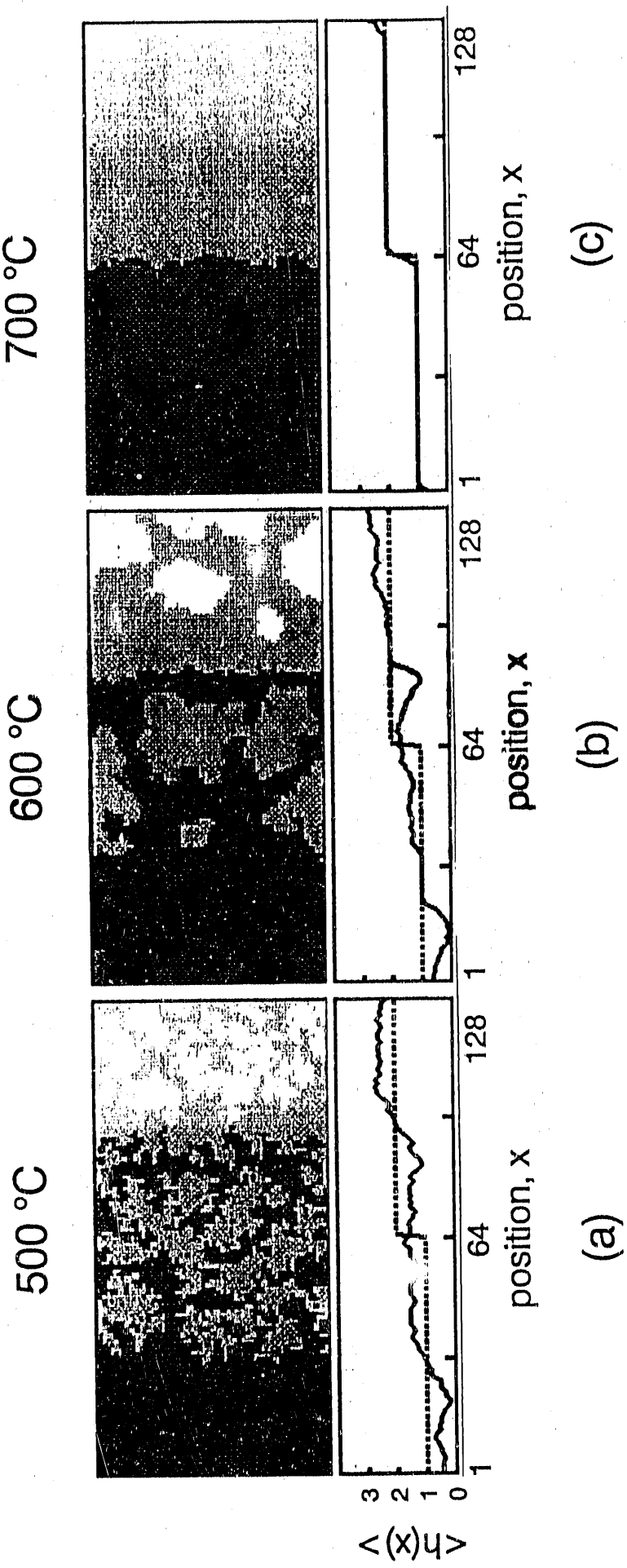


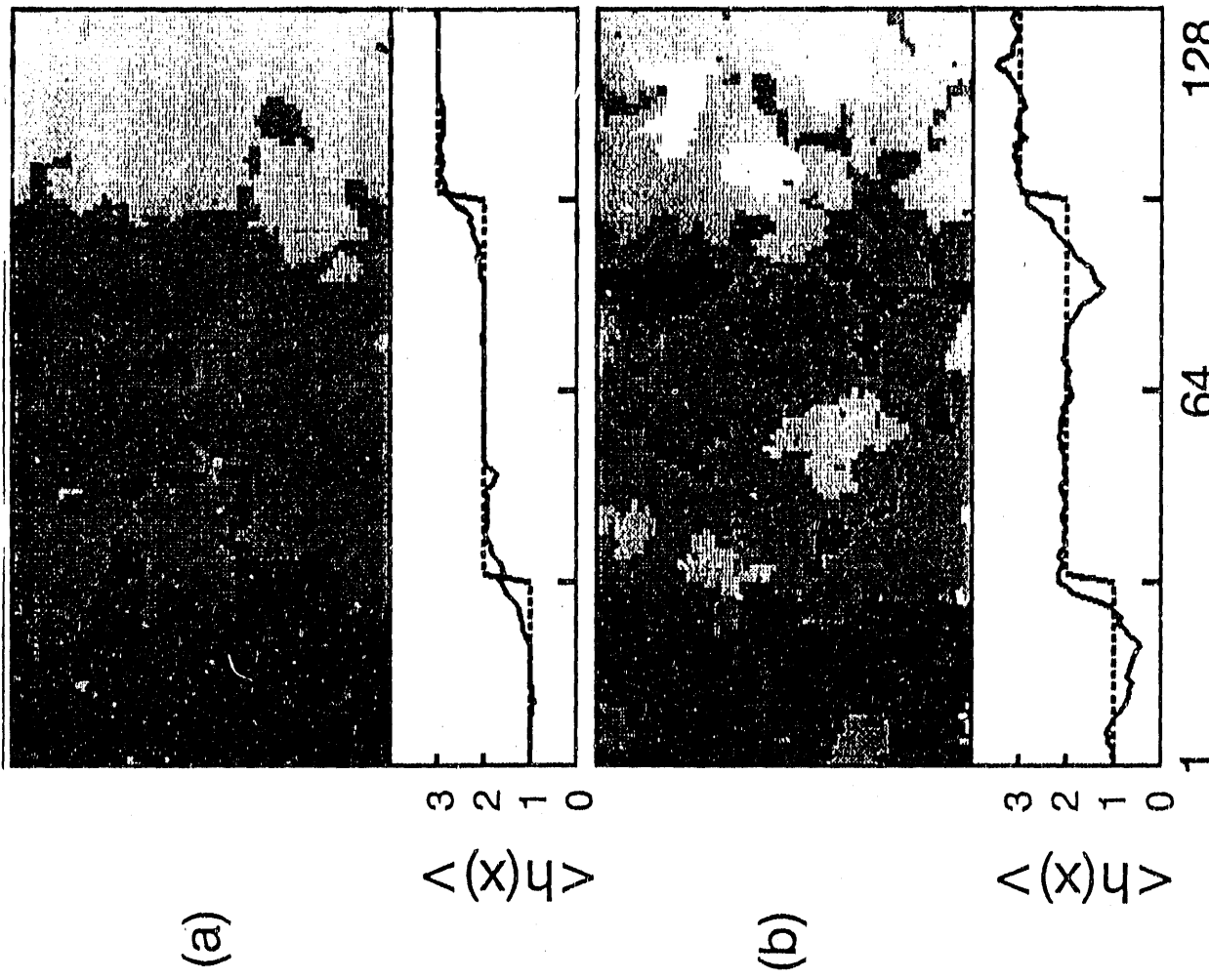
figure 2
Chason and Dodson
file: simul2.drw
AVS 1990

AVS 1990

Chason and Dodson
file: simul3.drw

figure 3

position, x



(a)

(b)

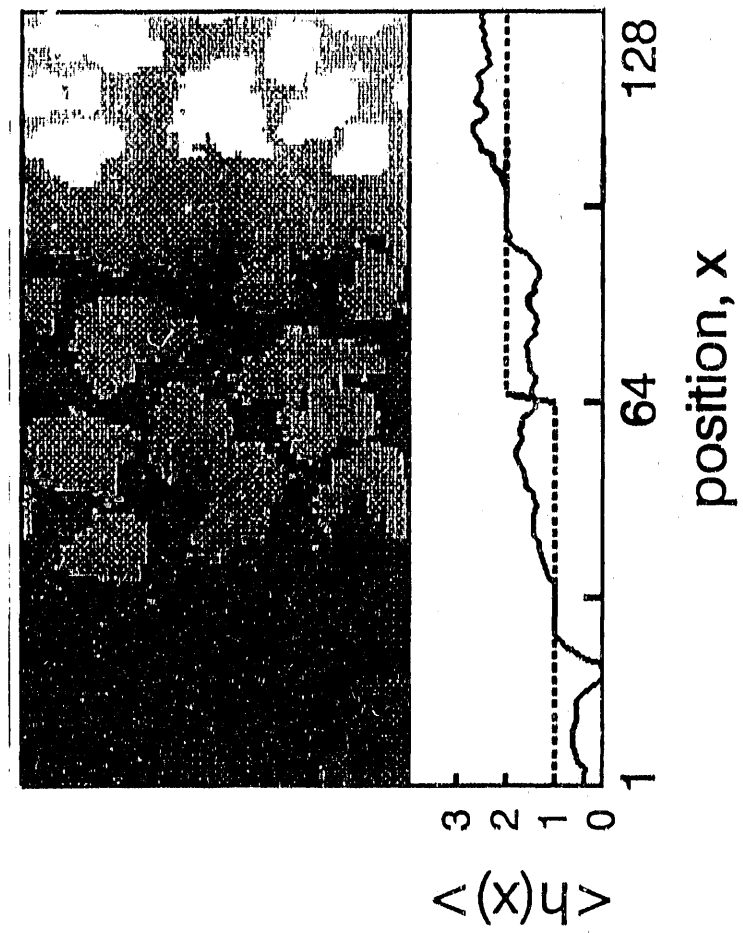


figure 4
Chason and Dodson
file: simul4.drw
AVS 1990

Isotropic Incorporation/Anisotropic Diffusion

500 °C, 0.5 monolayers

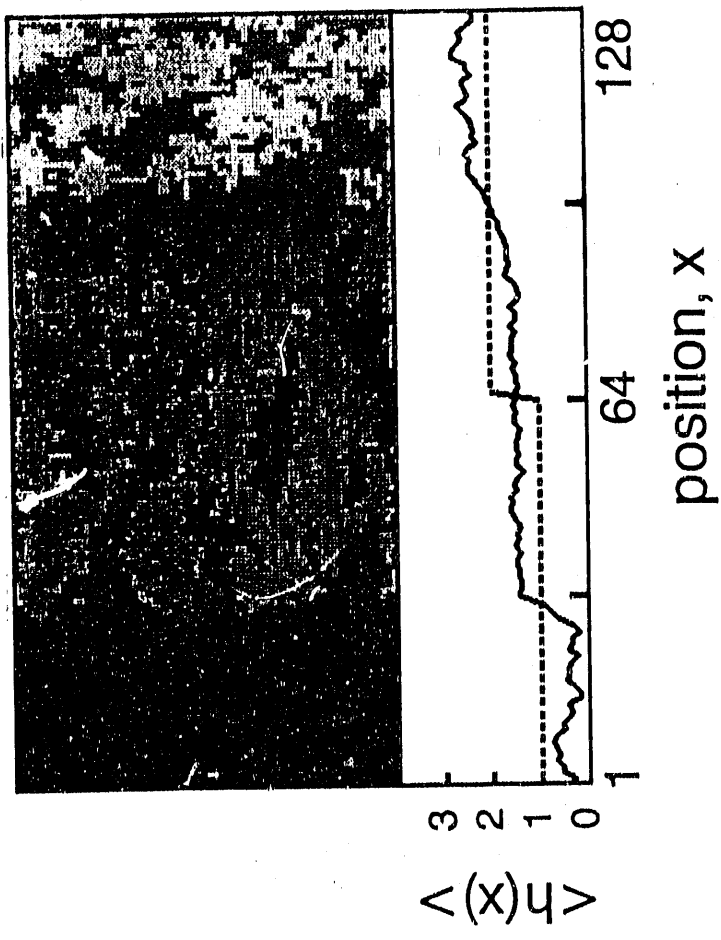


figure 5
Chason and Dodson
file: simul5.drw
AVS 1990

Anisotropic Incorporation and Anisotropic Diffusion (0.5 monolayers)

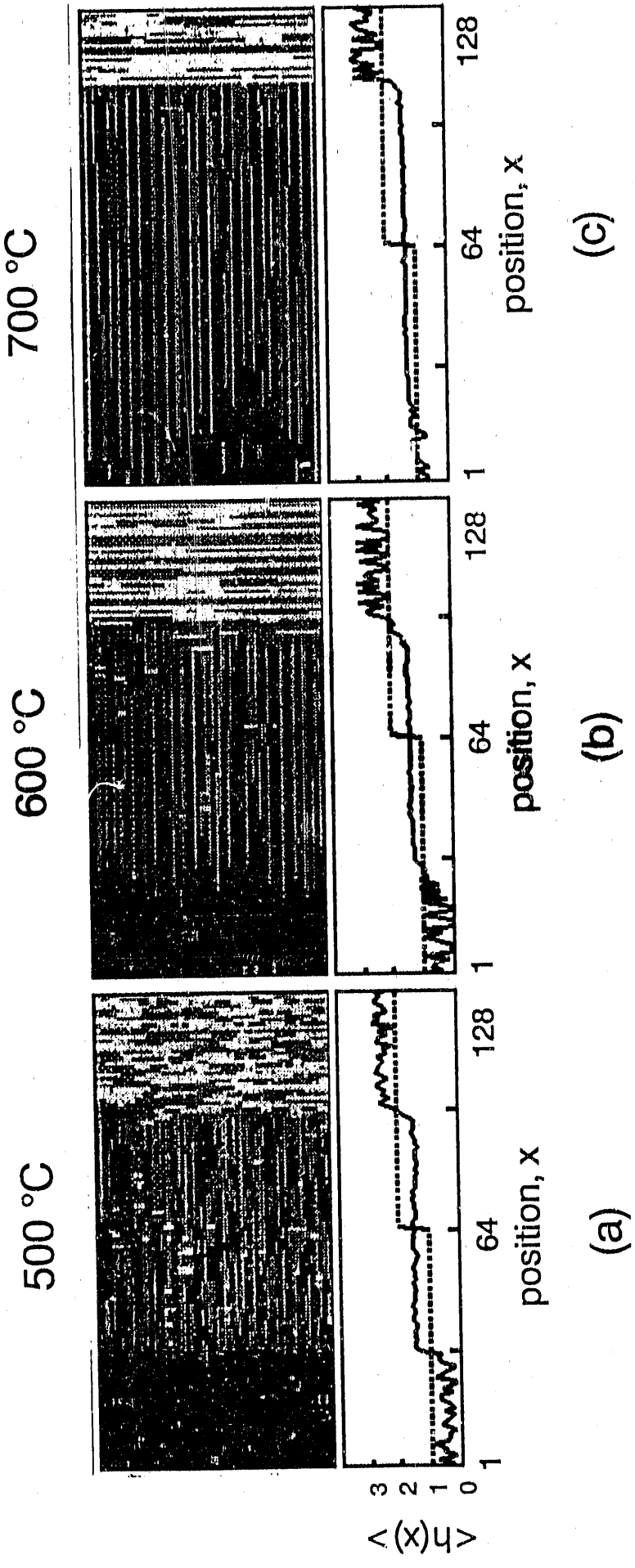


figure 6
Chason and Dodson
file: simul6.dnw
AVS 1990

END

DATE FILMED

11/08/90

